Original

SmtDNA: A Geant4-DNA User Application for Evaluating Radiation-induced Damage in Supercoiled Mitochondrial DNA

Tavakoli M. B.[1], Moradi H.[2]*, Khanahmad H.[3], Hosseini M.[4], Rahimmanesh I.[3]

[1]Department of Medical Physics and Medical Engineering, Isfahan University of Medical Sciences, Iran
[2]Department of Medical Physics, Kashan University of Medical Sciences, Iran
[3]Department of Genetics and Molecular Biology, Medical School, Isfahan University of Medical Sciences, Iran
[4]Department of Biostatistics and Epidemiology, School of Health, Isfahan University of Medical Sciences, Iran

ABSTRACT

Background: There is no geometrical nucleotide resolution model which can be used in numerical simulations of the interaction between radiation and supercoiled mt-DNA to perform realistic evaluations of DNA-free radical reactions.

Objective: A new geometrical model of mitochondrial DNA (mt-DNA) is developed in Geant 4-DNA to investigate the radiation-induced damage on mt-DNA. The presented application can be used to modify both geometrical parameters and structural elements, and to evaluate the damage induced on the mt-DNA molecule by ionizing particles.

Methods: Our model covers the organisation of a supercoiled human mitochondrial genetic system. The current model includes all 16,659 base pairs of human mitochondrial DNA. This new mtDNA model has been preliminarily tested in this work by determining SSB and DSB DNA damage yields and site-hit probabilities due to the impact of proton particles.

Results: Determination of single-strand (SSBs) and double-strand breaks (DSBs) is designed using the locations of all hit sites. Estimation of single-strand breaks and double strand breaks yielded similar results with the increment of incident particle LET. The output results contain the information about the energy transfers in the backbone region of DNA double helix.

Conclusion: Considerations seem to be consistent with the corresponding experimental determinations. This application can be used for the investigation of radiation-induced damage to the mitochondrial genome and in any problems that require a supercoiled geometrical model. This work is going to be extended to circular conformation in a parallel project in the near future.

Keywords

mt-DNA, Geometrical Model, Monte Carlo, Geant4, Radiation

Introduction

The main target of lesions induced by ionising radiation exposure is believed to be the genomic DNA in the cell nucleus [1]. Many studies have been conducted on the effects of radiation on cell organelles other than the nucleus [1-6]. It has been suggested that these organelle effects are not caused by the nuclear reaction to radiation but are due to the direct effect of radiation [1, 7]. Mitochondria may occupy approximately 30% of the total cell volume [8]. Ionising radiation can

*Corresponding author:
H. Moradi
Department of Medical Physics, Kashan University of Medical Sciences, Iran
E-mail: moradi_h@kaums.ac.ir

Received: 7 June 2017
Accepted: 1 july 2017

cause various lesions in circular mitochondrial DNA(mt-DNA) such as; strand breaks, base mismatches and large deletions, which also occur in nuclear DNA [1]. Therefore, mitochondria may also be a target of radiation, in addition to the cell nucleus [2]. Although, mt-DNA comprises approximately 0.25% of the total cellular DNA, the entire mitochondrial DNA includes active genes for protein synthesis [2, 9, 10]. In contrast, the portion responsible for protein coding in nuclear DNA (99.75% of the total cellular DNA) is only approximately 1% [9]. Consequently, the genetic cause of the direct biological effects seems to lie in the coding regions of mitochondrial DNA. In addition, Histone protection fails to efficiently protect mitochondrial DNA, and an efficient DNA repair system is inactive [4]; hence, more unrepaired lesions are likely to accumulate.

Human mt-DNA is a circular molecule among the smallest known mt-DNAs, and it contains 16,659 bases. The close proximity of mt-DNA to sites of reactive oxygen species (ROS) production renders it particularly susceptible to damage. Recent evidence has indicated that base excitation repair and mismatch repair might be induced in the mitochondria during oxidative insult [2]. Deletion in the mitochondrial genome is also commonly induced after cellular exposure to ionising radiation [11].

Geant4 is a general-purpose and open-source simulation toolkit which is well suited for microdosimetry purposes and radiation interactions in water [12, 13]. Various attempts have been made to predict early damages to DNA. Geant4-DNA can be utilized to address this problem in the following three steps: 1- using clustering algorithms to estimate the damages, 2- performing geometrical simulations of the structure and 3- using the first and second approaches together. Energy deposition patterns in media can be analysed and tuned to adapt to the experimental DNA strand break data using clustering algorithms [14, 15]. A clustering algorithm was added to the Geant4-DNA examples in December 2015 (Geant4.10.2). In geometrical approach, attempts were made to develop geometrical models of biological molecules. Using physical, chemical-physical and chemical-biological processes in combination with Geant4-DNA, physical modelling of a DNA geometrical structure in liquid water was first conducted by Bernal et al. [16]. The aim of their simulation was to estimate single- and double-strand breaks in a simplified DNA structure formed by a series of chromatin cylindrical forms, using some radionuclides, cobalt gamma rays or soft X-rays as the radiation sources. Attempts to describe 6Gbp in nuclear DNA started and continued in several research groups [17-22]. In most studies, authors focused on nuclear genome and tried to make theoretical and experimental investigations of radiation-induced damage on nuclear genome. Up to our knowledge, in theoretical approach, there is no investigation on supercoiled conformation of molecules. PDB4DNA package in Geant4-DNA was developed to simulate radiation effects on molecules within their Protein Data Base (PDB) files [23]; in contrast, there is no way to use it for mt-DNA because of the lack of PDB files in this case. This is why a specific-purpose model is being presented through this application.

In our study, we tried to develop a supercoiled model for mitochondrial genome to achieve a nucleotide resolution of the whole cell genome including mt-DNA. The low-energy package prepared in Geant4-DNA can be used to simulate the energy-deposition physics of ionising radiation at the nano-metric scale for radiobiological applications [24, 25]. Therefore, the mt-DNA geometries created in this study are directly exportable in a form suitable for the use in MC simulations using Geant4-DNA processes.

In this study, supercoiled mt-DNA model was developed using the Geant4 Monte Carlo simulation tool, considering the sugar and base-pair level of granularity. The structure of

the paper is as follows; first, we present the basic features of simulations of DNA molecule models with base-pair resolution, which are common to Geant4-DNA and other examples. Then, the specific characteristics of this application (those that serve to determine the structure) are discussed including visualisations of the structure by the Geant4 tools to clarify the description. Finally, the algorithm for assigning SSBs and DSBs to the mt-DNA geometry is proposed; this is used to compute an estimation of the mt-DNA damage.

Methods

SmtDNA can simulate energy deposition to base-pairs in supercoiled mt-DNA molecule and estimate the SSB and DSB damage. Users can visualise particle tracks using OGL tool in Geant4. Figure 1 presents the Unified Modelling Language (UML) diagram of the application in the Geant4 toolkit. Green boxes correspond to SmtDNA. Our model covers the organisation of a supercoiled human mitochondrial genetic system. Pairs should be separated by distances of 0.33 nm. An optimisation process is used to determine the geometrical dimensions of the structure. Bases and sugars are assumed to be spheres with radii of 0.17 nm and 0.48 nm, respectively, according to other studies [16]. The number of base pairs per complete rotation in a double helix is taken to be 10.3, which is the experimental value. Rotation takes place through a 3D rotation matrix with a rotation degree of 360°/10.3[16].

Determination of Supercoiled Geometrical Structure

Figure 2 shows the rotating structure with an expanded view of the supercoiled DNA system.

The geometric design, which includes two semicircles at the ends, and two spiral paths between them are divided into two steps:

1. The rotation of the two semicircle and the two spiral paths is obtained by using 3D rota-

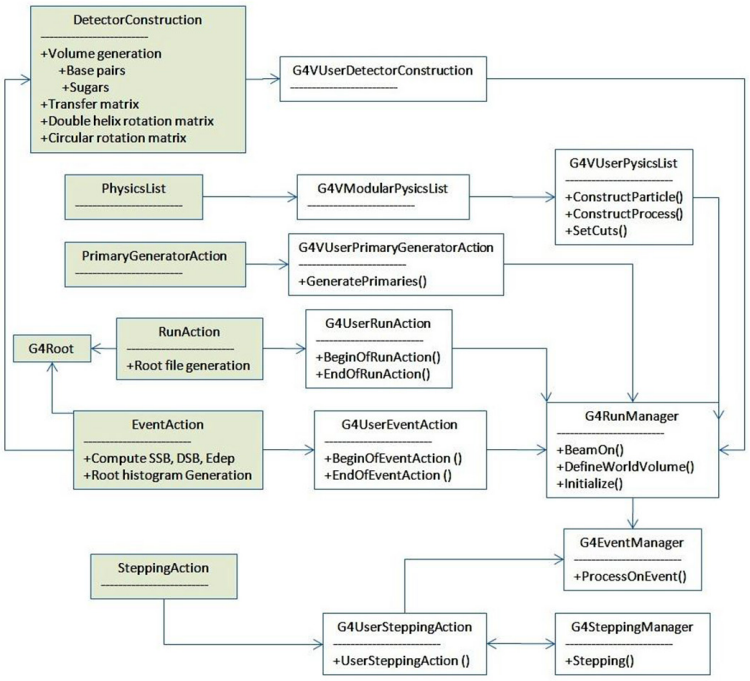

Figure 1: UML diagram of SmtDNA Geant4 user application: Geant4 virtual classes (white), Geant4 implemented classes and interface to the ROOT analysis software (green).

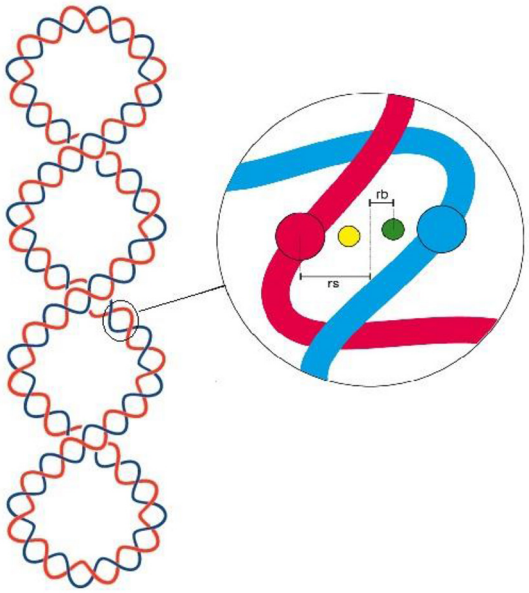

Figure 2: Rotating structure with an expanded view of the supercoiled DNA system.

tion matrixes for each path, which are multiplied by the previous rotation matrix in order to determine the permutation matrix. The entire supercoiled structure is formed by precisely localizing the starting points of the chains. Figure 3 shows a closer view of our model,

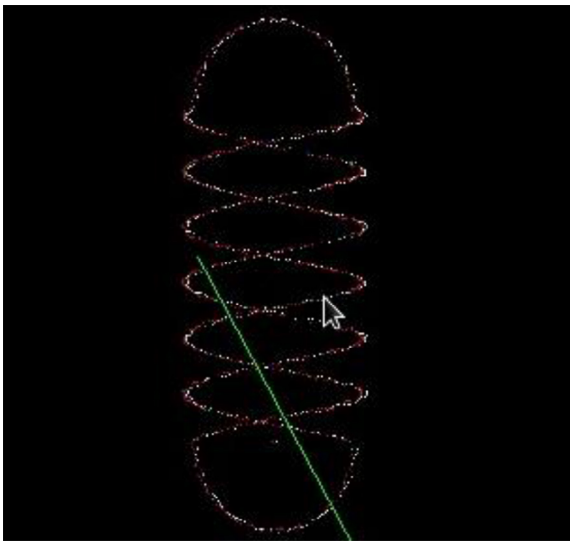

Figure 3: Visualisation of the supercoiled geometry, created by the OGL visualisation tool in Geant4.

which was obtained using the OGL tool in Geant4. A detail can be seen in Figure 4.

2. The mathematical algorithm for the geometric construction is described below, where *N1*= Number of elements in the first semicircle path, *N2*= Number of elements in the second semicircle path, *N3*= Number of elements in the first spiral path, *N4*= Number of elements in the second spiral path:

2-1. First, the two semicircles are built as follows:

$$SP_n = \begin{bmatrix} -rs\mathrm{Cos}(n\theta_0) & 0 & rs\mathrm{Sin}(n\theta_0) \\ rs\mathrm{Cos}(n\theta_0) & 0 & -rs\mathrm{Sin}(n\theta_0) \end{bmatrix}$$

The rotation matrix for the n^{th} element is written as:

$$Matrix_n = \begin{bmatrix} \mathrm{Cos}(n\varphi_0) & -\mathrm{Sin}(n\varphi_0) & 0 \\ \mathrm{Sin}(n\varphi_0) & \mathrm{Cos}(n\varphi_0) & 0 \\ 0 & 0 & 1 \end{bmatrix}, , \varphi_0 = \frac{2\pi}{\mathrm{Num}}$$

where n=0, 1, 2, … , number of elements in each supercoil path.

Thus, the permutation matrix for the n^{th} element is given by:

$$D_{nN} = \left[SP_{nN1} \times \mathrm{Matrix}_{nN1}\right]_{2\times 3} = \left[D^1_{nN1} \quad D^2_{nN1}\right]$$

The n^{th} spin, regardless of its permutation matrix, should have a geometrical coordinate transformation. Thus the parametric equation for the spin is:

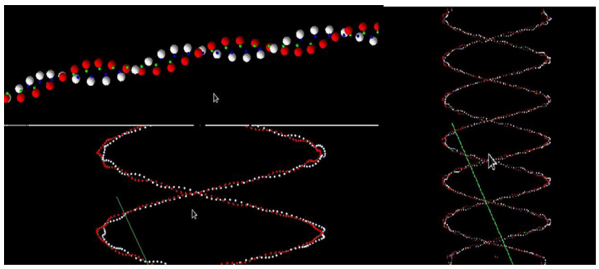

Figure 4: Closer views of the geometry.

$$P_{nN13}=\begin{cases}\begin{cases}x=rrCos(n\varphi_0)\\ y=rrSin(n\varphi_0)\\ z=z_0\end{cases} & ,0\le n<N1\\ \begin{cases}x=rrCos(n\varphi_0)\\ y=-rrSin(n\varphi_0)+2(b-a)\times 2\pi N\_N\\ z=z_0\end{cases} & ,N1\le n<N1+N3-1\end{cases}$$

and the location of the n^{th} element is given by:

$$\text{Sugar Location}_{nN13}=\left[D^1_{nN13}+P_{nN13}\quad D^2_{nN13}+P_{nN13}\right]$$

2-2. Up to this step, we have obtained the geometrical position of the two semicircles. The first spiral should be built using *N2* elements. Thus,

$$SP_{nN2}=\begin{bmatrix}-rs\text{Cos}\left((N1+n)\theta_0\right) & 0 & rs\text{Sin}\left((N1+n)\theta_0\right)\\ rs\text{Cos}\left((N1+n)\theta_0\right) & 0 & -rs\text{Sin}\left((N1+n)\theta_0\right)\end{bmatrix},$$

$$n=0,1,2,\ldots,(N2-1).$$

The rotation matrix for the n^{th} element is written as:

$$\text{Matrix}_{nN2}=\begin{bmatrix}\text{Cos}(n\varphi_0) & -\text{Sin}(n\varphi_0) & 0\\ \text{Sin}(n\varphi_0) & \text{Cos}(n\varphi_0) & 0\\ 0 & 0 & 1\end{bmatrix},\ \varphi_0=\frac{2\pi}{\text{Num}}$$

, *n*=0,1,2, … , (*N2*-1).

Thus, the permutation matrix for the n^{th} element is

$$D_{nN2}=\left[SP_{nN2}\times\text{Matrix}_{nN2}\right]_{2\times3}=\left[D^1_{nN2}\quad D^2_{nN2}\right].$$

The parametric coordinate transformation of the n^{th} element in the spiral path is given by:

$$P_{nN2}=\begin{cases}x=rrCos(ndt)\\ y=2(n+1)dt(b-a),dt=\dfrac{2\pi N\_N}{N2}.\\ z=rrSin(ndt)\end{cases}$$

Therefore, the location of the n^{th} element is

$$\text{Location}_{nN13}=\left[D^1_{nN12}+P_{nN12}\quad D^2_{nN12}+P_{nN12}\right]$$

and for the next spiral path, which has *N4* elements, we have

$$dt2=\frac{2\pi N\_N}{N4},$$

$$SP_{nN4}=\begin{bmatrix}-rs\text{Cos}\left((N1+N2+N3+n)\theta_0\right) & 0 & rs\text{Sin}\left((N1+N2+N3+n)\theta_0\right)\\ rs\text{Cos}\left((N1+N2+N3+n)\theta_0\right) & 0 & -rs\text{Sin}\left((N1+N2+N3+n)\theta_0\right)\end{bmatrix},$$

$$n=0,1,2,\ldots,(N4-1).$$

The rotation matrix for the n^{th} element is written as:

$$\text{Matrix}_{nN4}=\begin{bmatrix}\text{Cos}(n\varphi_0) & -\text{Sin}(n\varphi_0) & 0\\ \text{Sin}(n\varphi_0) & \text{Cos}(n\varphi_0) & 0\\ 0 & 0 & 1\end{bmatrix},\ \varphi_0=\frac{2\pi}{\text{Num}}$$

, n=0,1,2, … , (*N4*-1).

Thus, the permutation matrix for the n^{th} element is

$$D_{nN4}=\left[SP_{nN4}\times\text{Matrix}_{nN4}\right]_{2\times3}=\left[D^1_{nN4}\quad D^2_{nN4}\right]$$

The parametric coordinate transformation of the n^{th} element in the spiral path is given by:

$$P_{nN4}\begin{cases}x=rrCos(\pi-ndt2)\\ y=2(b-a)2\pi N\_N-2(n-1)dt2(b-a)\\ z=rrSin(ndt)\end{cases},dt2=\frac{2\pi N\_N}{N4}$$

Thus, the location of the n^{th} element is

$$\text{Location}_{nN4}=\left[D^1_{nN4}+P_{nN4}\quad D^2_{nN4}+P_{nN4}\right].$$

2-3. Now we calculate the locations of the base pairs in the first and second spiral paths. The placement of the first spiral path base pairs is given by:

$$b\_SP_{nN\,4}=\begin{bmatrix}-rb\mathrm{Cos}\left((N1+n)\theta_0\right) & 0 & rb\mathrm{Sin}\left((N1+n)\theta_0\right)\\ rb\mathrm{Cos}\left((N1+n)\theta_0\right) & 0 & -rb\mathrm{Sin}((N1+n)\theta_0\end{bmatrix},$$

n=0,1,2,…,(*N2*-1).

By assuming $dt=\frac{2\pi N\_N}{N2}$, the rotation and transfer matrices the same as for sugars. Hence, the permutation matrix for the n^{th} element is

$$b_{D_{nN\,2}}=\left[b_{SP\,nN\,2}\times \mathrm{Matrix}_{nN\,2}\right]_{2\times 3}=\left[b_{D\,nN\,2}^{1}\quad b_{D\,nN\,2}^{2}\right]$$

The parametric coordinate transformation for the n^{th} base pair in the spiral path is also the same as for sugars ($P_{nN\,2}$); thus, the location is

$$\mathrm{b\_Location}_{nN\,2}=\left[b\_D_{nN\,2}^{1}+P_{nN\,2}\quad b\_D_{nN\,2}^{2}+P_{nN\,2}\right]$$

2-4. In the second spiral, we have *N4* base pairs. The base pairs matrix would be

$$b_{SP_{nN\,4}}=\begin{bmatrix}-rb\mathrm{Cos}\left((N1+N2+N3+n)\theta_0\right) & 0 & rb\mathrm{Sin}\left((N1+N2+N3+n)\theta_0\right)\\ rb\mathrm{Cos}\left((N1+N2+N3+n)\theta_0\right) & 0 & -rb\mathrm{Sin}((N1+N2+N3+n)\theta_0\end{bmatrix}$$

, n=0,1,2,…,(*N4*-1).

By assuming $dt2=\frac{2\pi N\_N}{N4}$, the rotation and transfer matrix of base pairs is the same as $\mathrm{Matrix}_{nN\,4}$. Hence, the permutation matrix for the n^{th} element is

$$b_{D_{nN\,4}}=\left[b_{SP\,nN\,4}\times \mathrm{Matrix}_{nN\,4}\right]_{2\times 3}=\left[D_{nN\,4}^{1}\quad D_{nN\,4}^{2}\right]$$

The parametric coordinate transformation for the n^{th} base pair in the spiral path is the same as for sugars ($P_{nN\,4}$), thus the location is given by:

$$\mathrm{b\_Location}_{nN\,4}=\left[b\_D_{nN\,4}^{1}\quad b\_D_{nN\,4}^{2}\right].$$

Results

Geometry Consistency by Visualisation

Visualisation of a 0.1 MeV proton in interaction with an mt-DNA molecule and its water environment was checked as the first step (Figures 5). Then, the code was run with the complete number of base pairs in the molecular structure. The coordinates determined by the algorithm were consistent with the expected result, as shown in Figure 6, which are plotted using the ROOT software and show the hit sites in the exact structure for model. The results can be compared with those for any other arbitrary DNA shape, owing to the assumption of a standard supercoiled structure model in this study and the probabilistic nature of Monte Carlo calculations.

Algorithm for Evaluating SSBs and DSBs

A minimum energy deposition of 8.22 eV delivered to the sugar-phosphate sphere is assumed as SSBs. This minimum energy is the

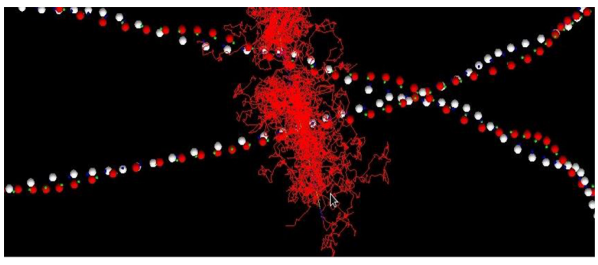

Figure 5: Visualisation of a 0.1 MeV proton in interaezdxction with a supercoiled mtDNA molecule and its water environment.

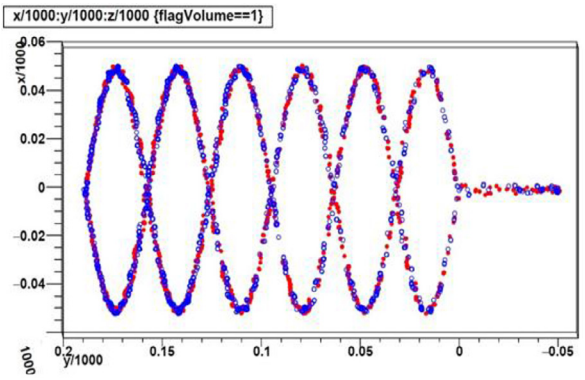

Figure 6: 3D analysis of the track position of the current energy transfer (in nm) for the supercoiled structure.

same in all Geant4-DNA models. DSBs are assumed when two SSBs occur on opposite sides of the molecule at a distance of 10 base-pairs or less (Figure 7). This parameter is obtained from the studies of Nikjoo et al. [26-28]and is also used in other Geant4 examples [22-23, 29-32].

Output Production

All ionisations produced by the projectile and the secondary electrons were recorded in a ROOT file format. The output file was processed by analysing the routines.

The output results are stored in an MtDNA. root file, containing only information about the energy transfers in the backbone region of the DNA double helix. The output file can be analysed by root analysing tools. The parameters reported in output root files are: 1-strand breaks, which are distinguished with different flags (1 or 2), 2- types of particles for the current step, 3- types of the processes for the current step, 4- flag of the strand (1 or 2) in the

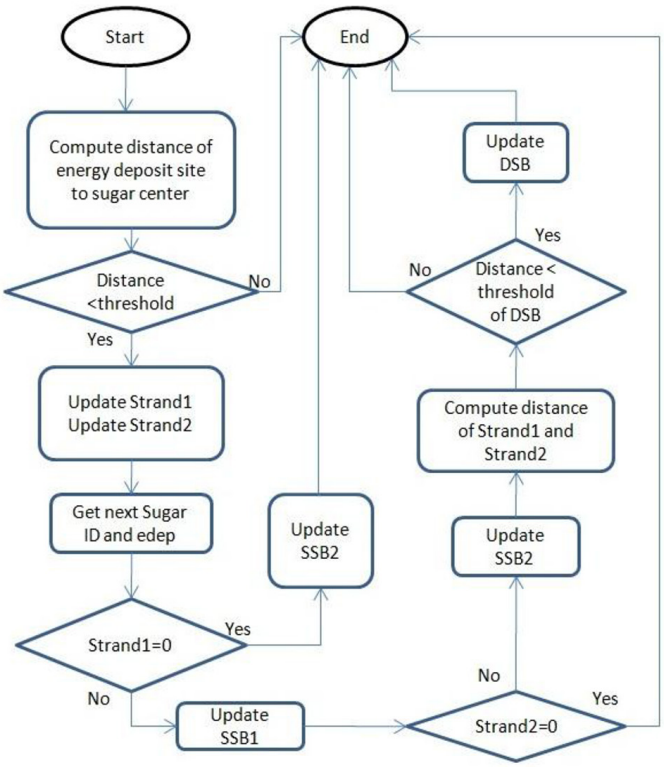

Figure 7: Activity diagram of the algorithm converting energy depositions into DNA strand breaks.

double helix, 5- track position of the current energy transfer (in nm) 6- 3D analysis of the track position of the current energy transfer (in nm), which is shown in Figure 6, 7- energy deposit corresponding to the energy transfer (in eV), 8-total energy loss along the current step (in eV) and 9- step length of tracks (in nm). Using these analysing options helps users to analyse their studies in advance.

SSBs and DSBs are calculated using our optimised algorithm, which is described by a UML diagram in Figure 7, as output to an MtDNA.out ASCII file.

Setup of Simulations

The simulation was tested for proton particles. Protons with 10 different energies (100, 200, 300, 400, 500, 600, 700, 800,900, 1×10^3, 2×10^3, 5×10^3, 1×10^4, 2×10^4, 5×10^4 and 1×10^5 keV) were emitted as primary particles. For the energy tracking, 105particles were simulated independently. A track is formed by all energy transfer points originating from the projectile and the secondary particles created by interactions. The target material was water.

Discussion

The aim of this study was to develop a nucleotide-resolution geometrical model of the supercoiled mt-DNA structure using the Geant4-DNA toolkit to predict radiation-induced damage such as SSBs, DSBs, energy deposition and some other physical parameters.

The current model includes all 16,659 base pairs of human mt-DNA. One should note that the primary purpose of this study was not to investigate all radiation-induced effects on mt-DNA, but to introduce two new geometrical models suitable for this purpose. The benchmarks of the model were compared with some other simulation and experimental studies.

Mean mtDNA Hit Number

In order to check the validation of the simulations in comparison with other simulations in this scope, total hit number probability was compared with Mylan et al. study in Dna-fabric project [21]. Figure 8 shows the mean number of mt-DNA hits proton for different energies in comparison with Dna-fabric tool. The results in both studies reveal the number of DNA hits decreases when the energy of incident proton increases.

LET and Hit Number

Figure 9 shows the relation between the linear energy transfer (LET) and the energy deposited in the mt-DNA. Indeed, DNA damage increases by increasing the LET. Our results are comparable with those obtained by Dos Santos et al., Bernal et al. and Souici et al. [18, 20, 33].

Energy and mt-DNA Hit Probability

Figure 10 demonstrates the relation between deposited energy and site-hit probability. The fact that the hit probability increases with increasing deposited energy is in agreement with the results of the experimental studies conducted by Zhou [28] and Souici [33, 34].

As shown in Figure 8, there is a decrease in the mean number of DNA hits with the energy. This trend was expected as an increase in energy corresponds to a decrease on LET.

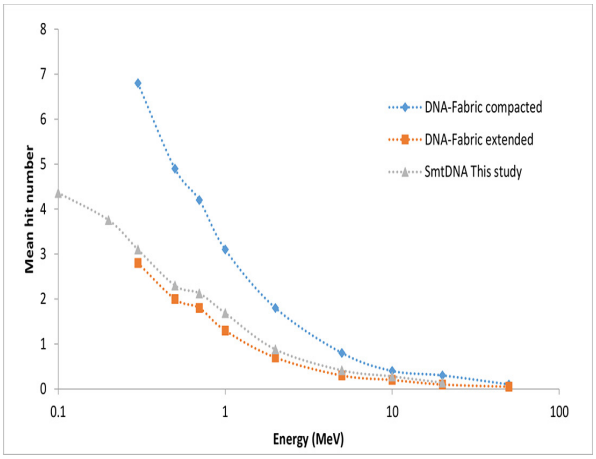

Figure 8: Mean number of hits per track.

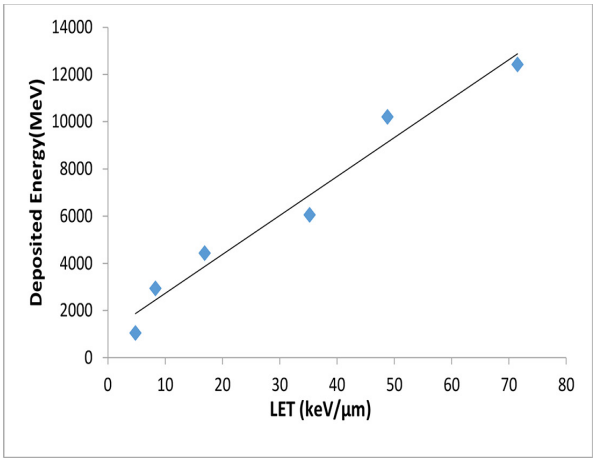

Figure 9: Relation between LET and deposited energy.

The plot of the mean number of DNA hits per track in Figure 9 also shows a larger mean hit number for low energies. As shown in Figure 10, the total amount of SSBs (i.e. of deposited energy) increases with increasing radiation LET. Indeed, an increase in the radiation LET increases the energy transfer point density of the tracks and, consequently, the probability to obtain an energy deposition on sensitive areas (backbone region), leading to an increase in DNA damage. We also observe that the

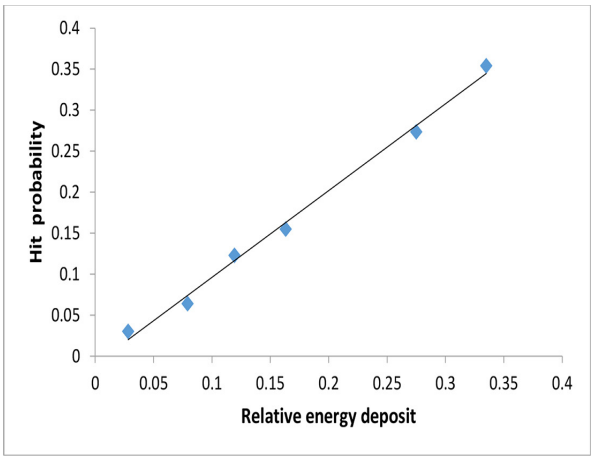

Figure 10: Relation between relative deposited energy and mt-DNA hit probability.

increase in the number of SSBs is more pronounced for protons between 0.5 and 2 MeV (41.9–16.9 keV/µm). As seen in Figure 11, the site hit probability increases with increasing deposited energy, in agreement with the experimental studies conducted by Zhou [28] and Souici [33, 34]; this reinforces the validation of the present code and allows a better understanding of the method by which fragmentation occurs when direct and indirect effects are taken into account.

Now, it is possible to use this code to obtain calculation evidence that suggest mtDNA fragmentation due to direct and indirect effects, which mainly occur as a consequence of proton track overlapping, or in other words, fragmentation occurs in the intersection areas of neighbouring proton tracks due to cumulative events. Moreover, a linear behaviour of the direct effects versus LET was also suggested by Dos Santos et al., who assessed the influence of chromatin density on the number of clustered damages created by protons for nuclear DNA.

The SSB and DSB calculations were performed through an optimised procedure that

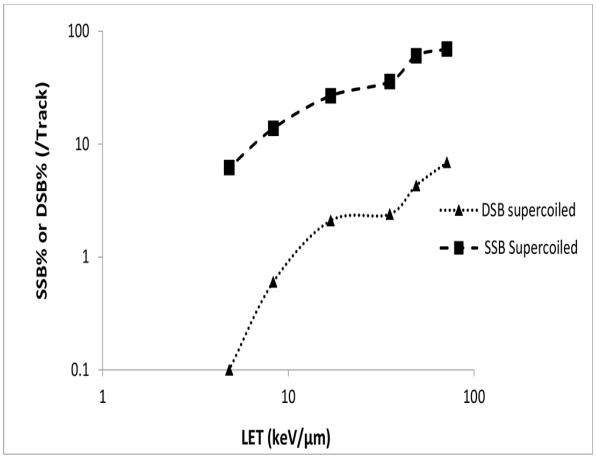

Figure 11: SSBs and DSBs as a function of linear energy transfer (LET) caused by proton irradiation in supercoiled structure.

uses all the output data on the interactions, which are stored in an MtDNA.root file. Our approach seems to be better than that of PDB4DNA example [23], which performs SSB and DSB calculations in each event and reflects the additive nature of DNA damage.

The mean number of SSBs per track for different energies and for the supercoiled mt-DNA geometry is shown in Figure 11. The results reveal that the number of SSBs decreases with increasing energy (or, equivalently, decreasing linear energy transfer (LET)) for all simulated energies.

Conclusion

This paper introduces the SmtDNA tool, a Geant4 application which includes a geometrical model to facilitate the study of mt-DNA radiation-induced damage. The model for base-pair resolution of human mt-DNA was developed based on the real data for the supercoiled mt-DNA structures. This new mt-DNA model has been preliminarily tested in this work by the visualisation and estimation of SSBs and DSBs produced by irradiation with protons of different energies. This model can be used in numerical simulations of the interaction between radiation and mt-DNA to perform realistic evaluations of DNA-free radical reactions. Attempts to extend this simulation tool to include other cytoplasm organelles are in progress.

Acknowledgment

This work is a part of a Ph.D. thesis supported financially by Isfahan University of Medical Sciences (Grant No.39396).

Conflict of Interest

None

References

1. Kam WW, Banati RB. Effects of ionizing radiation on mitochondria. *Free Radic Biol Med.* 2013;**65**:607-19. doi: 10.1016/j.freeradbiomed.2013.07.024. PubMed PMID: 23892359.
2. Azzam EI, Jay-Gerin JP, Pain D. Ionizing radiation-induced metabolic oxidative stress and prolonged cell injury. *Cancer Lett.* 2012;**327**:48-60. doi: 10.1016/j.canlet.2011.12.012. PubMed PMID: 22182453; PubMed Central PMCID: PMC3980444.
3. Kam WW, Lake V, Banos C, Davies J, Banati R. Apparent polyploidization after gamma irradiation: pitfalls in the use of quantitative polymerase chain reaction (qPCR) for the estimation of mitochondrial and nuclear DNA gene copy numbers. *Int J Mol Sci.* 2013;**14**:11544-59. doi: 10.3390/ijms140611544. PubMed PMID: 23722662; PubMed Central PMCID: PMC3709747.
4. Larsen NB, Rasmussen M, Rasmussen LJ. Nuclear and mitochondrial DNA repair: similar pathways? *Mitochondrion.* 2005;**5**:89-108. doi: 10.1016/j.mito.2005.02.002. PubMed PMID: 16050976.
5. Malik AN, Czajka A. Is mitochondrial DNA content a potential biomarker of mitochondrial dysfunction? *Mitochondrion.* 2013;**13**:481-92. doi: 10.1016/j.mito.2012.10.011. PubMed PMID: 23085537.
6. Yukawa O, Miyahara M, Shiraishi N, Nakazawa T. Radiation-induced damage to mitochondrial D-beta-hydroxybutyrate dehydrogenase and lipid peroxidation. *Int J Radiat Biol Relat Stud Phys Chem Med.* 1985;**48**:107-15. PubMed PMID: 3874177.
7. Somosy Z. Radiation response of cell organelles. *Micron.* 2000;**31**:165-81. PubMed PMID: 10588063.
8. Kam WW, McNamara AL, Lake V, Banos C, Davies JB, Kuncic Z, et al. Predicted ionisation in mitochondria and observed acute changes in the mitochondrial transcriptome after gamma irradiation: a Monte Carlo simulation and quantitative PCR study. *Mitochondrion.* 2013;**13**:736-42. doi: 10.1016/j.mito.2013.02.005. PubMed PMID: 23485772.
9. Consortium EP, Birney E, Stamatoyannopoulos JA, Dutta A, Guigo R, Gingeras TR, et al. Identification and analysis of functional elements in 1% of the human genome by the ENCODE pilot project. *Nature.* 2007;**447**:799-816. doi: 10.1038/nature05874. PubMed PMID: 17571346; PubMed Central PMCID: PMC2212820.
10. Clayton DA. Transcription and replication of mitochondrial DNA. **Hum Reprod.** 2000;**15 Suppl 2**:11-7. PubMed PMID: 11041509.
11. Prithivirajsingh S, Story MD, Bergh SA, Geara FB, Ang KK, Ismail SM, et al. Accumulation of the common mitochondrial DNA deletion induced by ionizing radiation. *FEBS Lett.* 2004;**571**:227-32. doi: 10.1016/j.febslet.2004.06.078. PubMed PMID: 15280047.
12. Agostinelli S, Allison J, Amako Ka, Apostola-

kis J, Araujo H, Arce P, et al. GEANT4-a simulation toolkit. *Nucl Instrum Methods Phys Res A.* 2003;**506**:250-303.

13. Allison J, Amako K, Apostolakis J, Araujo H, Dubois PA, Asai M, et al. Geant4 developments and applications. *IEEE Trans Nucl Sci*. 2006;**53**:270-8.
14. Francis Z, Incerti S, Ivanchenko V, Champion C, Karamitros M, Bernal MA, et al. Monte Carlo simulation of energy-deposit clustering for ions of the same LET in liquid water. *Phys Med Biol*. 2012;**57**:209-24. doi: 10.1088/0031-9155/57/1/209. PubMed PMID: 22156022.
15. George NP, Ngo KV, Chitteni-Pattu S, Norais CA, Battista JR, Cox MM, et al. Structure and cellular dynamics of Deinococcus radiodurans single-stranded DNA (ssDNA)-binding protein (SSB)-DNA complexes. *J Biol Chem.* 2012;**287**:22123-32. doi: 10.1074/jbc.M112.367573. PubMed PMID: 22570477; PubMed Central PMCID: PMC3381170.
16. Bernal MA, Sikansi D, Cavalcante F, Incerti S, Champion C, Ivanchenko V, et al. An atomistic geometrical model of the B-DNA configuration for DNA-radiation interaction simulations. *Computer Physics Communications*. 2013;**184**:2840-7.
17. Incerti S, Douglass M, Penfold S, Guatelli S, Bezak E. Review of Geant4-DNA applications for micro and nanoscale simulations. *Phys Med*. 2016;**32**:1187-200. doi: 10.1016/j.ejmp.2016.09.007. PubMed PMID: 27659007.
18. Bernal M, Sikansi D, Cavalcante F, Incerti S, Champion C, Ivanchenko V, et al., editors. Performance of a new atomistic geometrical model of the B-DNA configuration for DNA-radiation interaction simulations. *J Phys Conf Ser*. 2014;**490**:012150.
19. Bueno M, Schulte R, Meylan S, Villagrasa C. Influence of the geometrical detail in the description of DNA and the scoring method of ionization clustering on nanodosimetric parameters of track structure: a Monte Carlo study using Geant4-DNA. *Phys Med Biol.* 2015;**60**:8583-99. doi: 10.1088/0031-9155/60/21/8583. PubMed PMID: 26501434.
20. Dos Santos M, Clairand I, Gruel G, Barquinero JF, Incerti S, Villagrasa C. Influence of chromatin condensation on the number of direct DSB damages induced by ions studied using a Monte Carlo code. *Radiat Prot Dosimetry*. 2014;**161**:469-73. doi: 10.1093/rpd/ncu029. PubMed PMID: 24615262.
21. Meylan S, Vimont U, Incerti S, Clairand I, Villagrasa C. Geant4-DNA simulations using complex DNA geometries generated by the DnaFabric tool. *Comput Phys Commun*. 2016;**204**:159-69.
22. Tajik M, Rozatian AS, Semsarha F. Calculation of direct effects of 60Co gamma rays on the different DNA structural levels: A simulation study using the Geant4-DNA toolkit. *Nucl Instrum Methods Phys Res B*. 2015;**346**:53-60.
23. Delage E, Pham QT, Karamitros M, Payno H, Stepan V, Incerti S, et al. PDB4DNA: Implementation of DNA geometry from the Protein Data Bank (PDB) description for Geant4-DNA Monte-Carlo simulations. *Comput Phys Commun*. 2015;**192**:282-8.
24. Incerti S, Baldacchino G, Bernal M, Capra R, Champion C, Francis Z, et al. The geant4-dna project. *International Journal of Modeling, Simulation, and Scientific Computing.* 2010;**1**:157-78. doi: 10.1142/S1793962310000122.
25. Karamitros M, Incerti S, Champion C. 376 the geant4-DNA project. *Radiother Oncol*. 2012;**102**:S191-S2.
26. Nikjoo H, O'Neill P, Terrissol M, Goodhead DT. Quantitative modelling of DNA damage using Monte Carlo track structure method. *Radiat Environ Biophys*. 1999;**38**:31-8. PubMed PMID: 10384953.
27. Nikjoo H, O'Neill P, Goodhead DT, Terrissol M. Computational modelling of low-energy electron-induced DNA damage by early physical and chemical events. *Int J Radiat Biol*. 1997;**71**:467-83. PubMed PMID: 9191891.
28. Nikjoo H, Emfietzoglou D, Watanabe R, Uehara S. Can Monte Carlo track structure codes reveal reaction mechanism in DNA damage and improve radiation therapy? *Radiation Physics and chemistry.* 2008;**77**:1270-9.
29. Tajik M, Rozatian AS, Semsarha F. Simulation of ultrasoft X-rays induced DNA damage using the Geant4 Monte Carlo toolkit. *Nucl Instrum Methods Phys Res B*. 2015;**342**:258-65.
30. Semsarha F, Raisali G, Goliaei B, Khalafi H. Microdosimetry of DNA conformations: relation between direct effect of (60)Co gamma rays and topology of DNA geometrical models in the calculation of A-, B- and Z-DNA radiation-induced damage yields. *Radiat Environ Biophys.* 2016;**55**:243-54. doi: 10.1007/s00411-016-0644-7. PubMed PMID: 26984469.
31. Semsarha F, Goliaei B, Raisali G, Khalafi H, Mirzakhanian L. An investigation on the radiation sensitivity of DNA conformations to 60Co gamma rays by using Geant4 toolkit. *Nucl Instrum Methods Phys Res B*. 2014;**323**:75-81.
32. Raisali G, Mirzakhanian L, Masoudi SF, Semsarha F. Calculation of DNA strand breaks due to direct and indirect effects of Auger electrons from incorporated 123I and 125I radionuclides using the Geant4 computer code. *Int J Radiat Biol*. 2013;**89**:57-64. doi: 10.3109/09553002.2012.715785. PubMed

PMID: 22892102.

33. Souici M, Khalil TT, Muller D, Raffy Q, Barillon R, Belafrites A, et al. Single- and Double-Strand Breaks of Dry DNA Exposed to Protons at Bragg-Peak Energies. *J Phys Chem B.* 2017;**121**:497-507. doi: 10.1021/acs.jpcb.6b11060. PubMed PMID: 28045263.
34. Zhou X, Liu X, Zhang X, Zhou R, He Y, Li Q, et al. Non-randomized mtDNA damage after ionizing radiation via charge transport. *Sci Rep*. 2012;**2**:780. doi: 10.1038/srep00780. PubMed PMID: 23110249; PubMed Central PMCID: PMC3483021.